

Reduction of Metal Oxide Particles with Syngas for Hydrogen Production

Velazquez-Vargas, L. G.; Li, F.; Gupta, P.; Fan, L.-S*
140 W. 19th Avenue, Columbus Ohio, 43210

Abstract

The understanding of the reduction mechanisms of metal oxide particles with syngas is important for the designing of the Syn Gas Redox (SGR) process. In the SGR process, composite particles of iron oxide are reduced in a moving bed reactor with syngas producing a sequestration ready CO₂ stream. Subsequently, the reduced particles are partially oxidized in a second reactor with steam to produce hydrogen. Finally, the particles are oxidized with oxygen before they are cycled back into the first reactor. In the SGR process, the heat liberated by the oxidation of the particles with steam and oxygen is used for the production of the high temperature steam. The heat integration of the SGR process leads to an estimated hydrogen production efficiency range of 70-75% (HHV).

Coal derived syngas usually contains various gases with its majority being carbon monoxide and hydrogen. To better understand the reduction of iron oxide composite particles, in this work, hydrogen gas was used as a reducing agent. Based on the kinetic data obtained, a diffusion–surface reaction kinetic model was developed. Further, a countercurrent moving bed reactor model was developed for the reduction of iron oxide with hydrogen. An industrial scale reactor was simulated and its performance was studied for various reactor lengths. It was found that, after a critical value, the increase in reactor length does not have a significant effect on the final conversion for gas and solids. This was explained by the formation of a near dead zone in the middle of the bed where the gas and solids reach a pseudo-equilibrium.

1. Introduction

Due to the rising of natural gas and crude oil prices encounter recently along with the increasing demand for hydrogen, the production of hydrogen from coal has received great interest. New gasification processes with higher hydrogen production efficiencies are being explored. One of such process is the Syngas Redox (SGR) process [Fan et al, 2005, 2006a-c]. Figure 1 shows a simplified schematic of the process, in which coal derived syngas is oxidized to carbon dioxide and water in a moving bed of iron oxide composite particles. This reduces the iron oxide to its metallic form. The reduced particles are then introduced into a second reactor where they react with high temperature steam producing a pure hydrogen stream. Subsequently, the partially oxidized particles are oxidized with oxygen liberating heat which is used to produce steam. After the particles are completely oxidized they are cycled back to the first reactor. The estimated hydrogen production efficiency for the SGR process can be as high as 75% [Velazquez-Vargas et al. 2006]. This efficiency is substantially higher than the gasification-Water Gas Shift (WGS) route with an estimated efficiency of 64% [Simbeck, 2002; Stiegel, 2006].

In the conventional gasification-WGS approach, hydrogen is produced by shifting the carbon monoxide contained in the syngas to carbon dioxide and hydrogen through a series of catalytic packed bed reactors. After the shift reaction the carbon dioxide is separated from the hydrogen and the remaining carbon monoxide through an expensive and energy intensive amine process [Herzog, 1999]. This separation process reduces the efficiency of the WGS process and increases the capital investment of the plant. In the SGR process, on the other hand, the carbon dioxide comes separated from the hydrogen by design. Hence, the carbon dioxide, after compression, can be sent to sequestration. Since 75% of the cost

* Corresponding Author. Tel.: +1-614-688-3262. E-mail.: fan.l@osu.edu

associated to the carbon management (being capture, transportation and sequestration) is associated to the separation of CO₂, the SGR process may be more attractive for the production of hydrogen at large scale in a central facility.

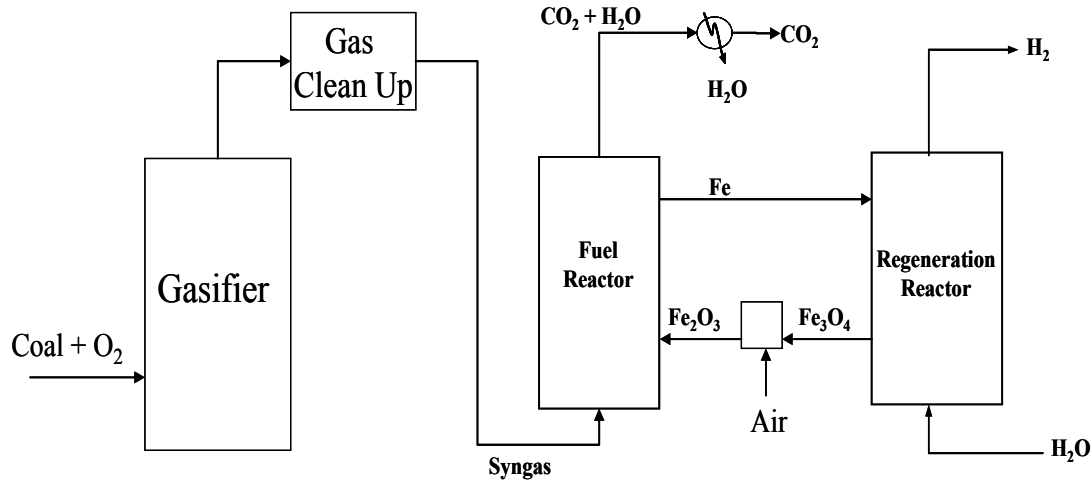


Figure 1. Schematic of the Syngas Redox process for hydrogen production from coal.

The work described in this paper focus in the development of a reduction kinetic model of iron oxide composite particles. The understanding of the reduction process of the iron oxide composite particles is important for the designing of the SGR reactors. Although, carbon monoxide is found in larger quantities in the syngas, the reduction of iron oxide with carbon monoxide may lead to the formation of undesired products (iron carbides) or carbon deposition by the well known reverse Boudard reaction (Reaction 1). Hence, for the sake of simplicity, hydrogen was chosen as the reducing agent.



The reduction of iron ores with hydrogen has been extensively investigated in the past, especially for the direct reduction of iron ores in the iron making industry [Turkdogan E. T. & Vinters, J. V., 1971]. However, the reduction of iron oxide with hydrogen is not simple. It is believed that iron oxide reduces in series from hematite to metallic iron passing through magnetite and Wustite [Nabi, G. & Lu, W-K. 1968] Many researchers believed that the reduction of hematite is controlled by the rate of diffusion and reaction of hydrogen into the particles [Spitzer, R.H. et al., 1968]. However, new evidence show that the reduction of iron oxide may be better modeled by the rate of diffusion of ionic oxygen out of the particle.

In this work, the reduction of iron oxide composite particles was model based on the diffusivity of oxygen out of the particles. Based on this model, a moving bed reactor model for the isothermal reduction of iron oxide with hydrogen was constructed. A reactor, designed for the production of 300 MW_{thermal} hydrogen production plant, was simulated. This simulation, although do not include the effects of carbon monoxide or other gases in the syngas, can be employed, as a first estimate, to evaluate the behavior of an industrial scale reactor. The reactor performance for various reactor lengths was studied.

2. Experimental Setup

The kinetic experiments were carried out in a fixed bed reactor operated in a differential reaction mode. The reactor setup consisted of a quartz tube of 6 mm ID with provision for pre-heating the gas before they contact the solid sample. A schematic diagram of the reactor set up is shown in Figure 2. The solid samples, between 200 to 250 mg, were placed in the middle of the heated section. The gas composition was controlled by manual mass flow controllers which control the amount of different gases sent to the reactor. The gas exiting the reactor was then sent to vent or to analysis. Gas analysis was performed using a microGC (Variant 4900). Once the reaction was completed, the reacting gas was switched to bypass and the reactor was flushed with inert gas. The solid samples were then taken out and placed in an inert atmosphere to cool down to room temperature.

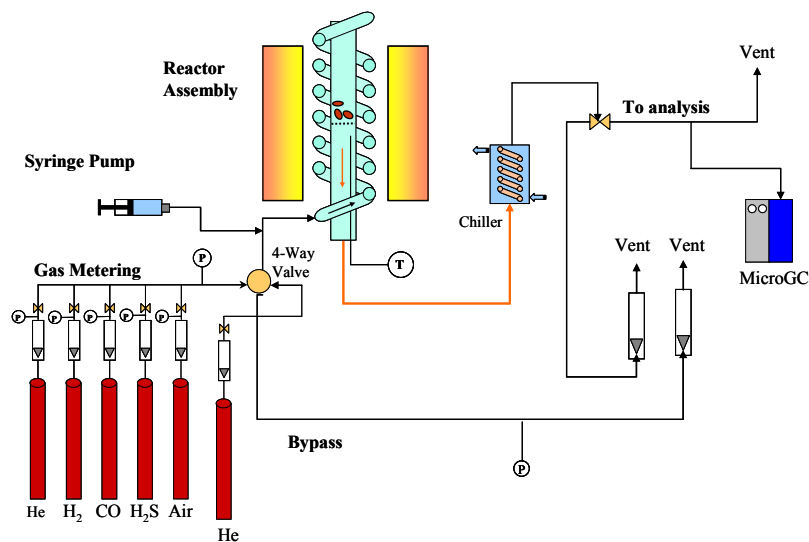


Figure 2. Experimental setup for kinetic experiments.

3. Kinetic Data

Reaction kinetic data was obtained by introducing approximately 0.15 to 0.25 g of iron oxide composite particles. Pellets of approximately 1 mm in diameter were meshed previously in order to obtain a narrow particle size distribution between each sample. The pellets were introduced, one batch at a time, into the reactor and reacted with hydrogen at 750 °C for a given length of time. Hydrogen concentration ranged from 5 to 20 % v/v. The total gas flow rate was kept at 1 L/min, which is validated to be above the critical flow value in order to minimize the mass transfer limitations due to the gas film layer diffusion. The particles that came out from the reactor were analyzed by measuring the weight change in a microbalance. Particle conversion here is defined as the amount of oxygen depleted from the particle at a given time divided by the total transferable oxygen contained in the particle. A particle with zero conversion means a fresh iron oxide composite particle and a fully converted particle (conversion=1) means that all the Fe₂O₃ contained in the particle is reduced to metallic iron. The conversion was calculated by equation 2:

$$\text{Conversion} = \frac{W_{\text{Initial}} - W_{\text{Final}}}{W_{\text{Initial}}} \frac{100}{X_{\text{Max}}} \quad (2)$$

where W_{Initial} is the initial weight of the particle (non-reacted). W_{Final} is the weight of the partially reacted particle. X_{Max} is the maximum weight drop percentage of a fully reduced particle. Figure 3 shows the particle conversion as a function of reaction time.

4. Kinetic Model

For particles with low surface area where the diffusion of gaseous reactants is limited, the reduction (or oxidation) is most likely to occur by an ionic transport mechanism. A reaction kinetics model was constructed based on the hypothesis that iron oxide reduction is limited by the oxygen ionic transport within the particle. Assuming that the diffusion of the oxygen ions is given by the Ficks' first law of diffusion, we can write the diffusion of oxygen atoms within the crystal lattice as:

$$J_o = -DC_{0,\text{initial}} \frac{\partial S}{\partial r} \quad (3)$$

The proposed reaction mechanism for the reduction of the iron oxide composite particles with hydrogen is as follows: the exchangeable oxygen, which is contained in the particle, diffuses to the surface of the particle where it reacts with the hydrogen to form water by the following reaction:



The electrons generated can then be transported back to the interior of the particle where they react with the ferric or ferrous ions giving ferrous or iron ions respectively. These reactions can be better seen as:



or



Based on these assumptions, the oxygen concentration in the particles is given by:

$$\frac{\partial S}{\partial \tau} = \frac{1}{\xi^2} \frac{\partial}{\partial \xi} \left(\xi^2 \frac{\partial S}{\partial \xi} \right) \quad (7)$$

With initial condition,

$$\text{at } \tau = 0 \quad \text{as} \quad S = 1 \quad (8)$$

and boundary condition as:

$$\text{for } \xi = 0 \quad \text{we have that} \quad \frac{\partial S}{\partial \xi} = 0 \quad (9)$$

and

at $\xi=1$ we have that
$$\frac{\partial S}{\partial \xi} = \theta \left(y_{H_2} - \frac{y_{H_2O}}{Ke} \right) S \quad (10)$$

with the following dimensionless groups.

$$y_{H_2} = \frac{P_{H_2}}{P_{H_2,Bulk}} \quad (11)$$

$$y_{H_2O} = \frac{P_{H_2O}}{P_{H_2,Bulk}} \quad (12)$$

$$S = \frac{C_O}{C_{O,Initial}} \quad (13)$$

$$\xi = \frac{r}{R_p} \quad (14)$$

$$\tau = \frac{Dt}{R_p^2} \quad (15)$$

and

$$\theta = \frac{R_p}{R T} \left(\frac{k}{D} P_{H_2,Bulk} \right) \quad (16)$$

The particle conversion was defined by the average concentration of the transferable oxygen at any given time. The conversion can be then calculated by:

$$\chi = 1 - 3 \int_0^1 S \xi^2 d\xi \quad (17)$$

The oxygen concentration was obtained by solving equations 7-10 and 17 using an explicit finite difference method. The radial ($d\xi$) and time ($d\tau$) dimensionless steps were chosen using the following equations:

$$d\xi = 0.1 \left(\frac{1}{\theta} \right) \quad (18)$$

and

$$d\tau = 0.01 \left(\frac{\tau_{final}}{\theta} \right)^2 \quad (19)$$

The experimental data was fitted using a multi-parameter, predictive, corrective, non-linear optimization method with an objective function given by:

$$\text{Error} = \sum_i \left(\frac{X_{\text{exp},i} - X_{\text{Model},i}}{X_{\text{exp},i}} \right) \quad (23)$$

where i is the number of experimental data points. The tolerance used was 1×10^{-6} .

The effect of the gas composition on the particle reduction with hydrogen at 750°C is shown in Figure 3. As can be seen the rate of reaction increases at higher hydrogen concentrations. For example, it can be observed in Figure 3 that particles reacting under 5% hydrogen conversion reach full conversion around 30 minutes, while particles with double concentration reach full conversion around 15 minutes, half the time. Similar effect can be seen when increasing the concentration even further to 20% hydrogen. In fact, according to the data and following the *initial rates method* [Fogler, 1999], the reaction was calculated to follow a first order with respect to hydrogen.

Figure 3 also shows a comparison between the experimental and the predicted conversion by the model. The solid lines represent the curve obtained by solving the kinetic model (Equations 7-10,17). As can be seen the model predicts well the experimental data for various hydrogen concentrations. Hence, this model can be used to predict the rate of reaction as a function of particle conversion to be used in a moving bed reactor model.

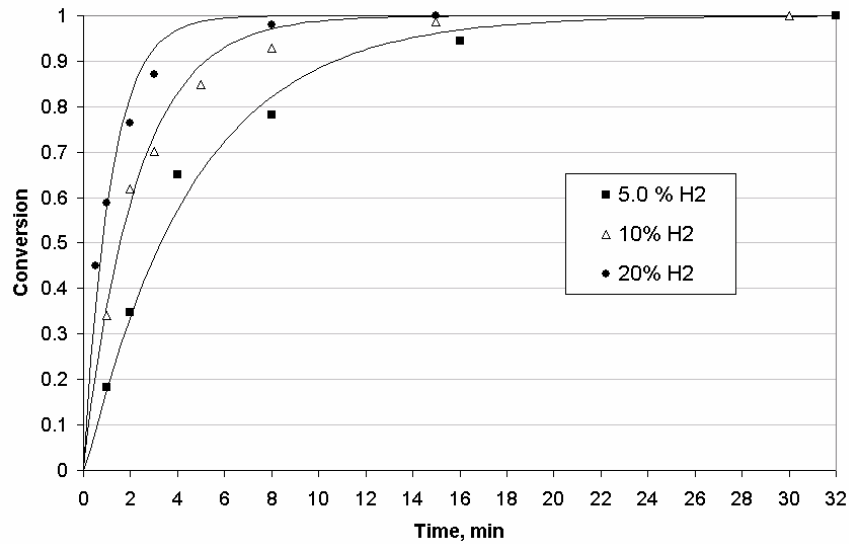


Figure 3. Reduction of iron oxide composite particles with hydrogen at 750°C ; Particle conversion as a function of time for various hydrogen concentrations.

5 Moving bed simulation model

Once the intrinsic kinetic rate model was obtained, a simulation of the moving bed reactor with countercurrent flow of gas and solid was conducted. In this model, the following assumptions were made:

1. The reactor is operated isothermally.
2. The gas and solid flows follow a plug flow behavior.
3. There is no concentration gradients in the radial direction.
4. The particles density is constant and particles are spherical with uniform particle size.

Figure 6 shows the operation of the countercurrent moving bed reactor. As can be seen, the solids are introduced from the top, with a mass flow rate equal to W_s and they are withdrawn from the bottom of the reactor. On the other hand, the gaseous reactants are introduced from the bottom with a volumetric flow rate equal to V and they are withdrawn from the top. The total length of the reactor is equal to L . A mass balance on a differential cross section of the reactor gives the following equations:

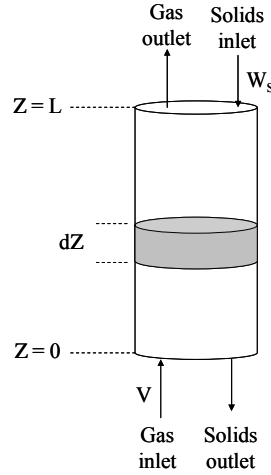


Figure 6. Illustration of the steady state operation of the countercurrent reduction reactor

For the solids,

$$\frac{\partial \chi}{\partial Z} = -A \left(\frac{\partial \chi}{\partial \tau} \right) \quad (24)$$

and for the gaseous species,

$$\frac{\partial y_{H_2}}{\partial Z} = -B \left(\frac{\partial \chi}{\partial \tau} \right) \quad (25)$$

$$\frac{\partial y_{H_2O}}{\partial Z} = B \left(\frac{\partial \chi}{\partial \tau} \right) \quad (26)$$

where

$$A = \frac{A_C L \rho_s}{W_s} (1 - \varepsilon) \quad (27)$$

and

$$B = \frac{A_C L}{V} \frac{R T}{P_t} (1 - \varepsilon) C_{0,initial} \quad (28)$$

with the following boundary conditions

$$\text{at } Z=0 \text{ we have that } y_{\text{H}_2} = y_{\text{H}_2,\text{initial}} \quad (29)$$

$$\text{and at } Z=1 \text{ we have that } \chi = 0 \quad (30)$$

6 Numerical Solution to the Moving Bed Reactor Model

The above moving bed model was solved using a finite difference method. Due to the countercurrent operation, the boundary conditions are found in two different location of the reactor. Hence, an initial guess on the solid conversion profile was introduced. The gas profile was then integrated in the upward direction followed by the solid profile in the downward direction. This process continued until the change in the gas and solid concentration profiles with respect to the previous iteration was less or equal to a tolerance value of 1e-6. The equilibrium constant, K_e , specific for each reaction according to the iron phase present was calculated using a thermodynamic software HSC Chemistry which uses thermochemical data available in literature [Chase M.W., 1998].

7 Model prediction

An industrial moving bed reactor for the reduction of iron oxide with hydrogen was simulated. The amount of solid processed in the reactor corresponds to a hydrogen production plant of 300 MW_{thermal}¹ with an overall efficiency of 75% (HHV). The diameter of the reactor was kept constant at 3.5 m while the length of the reactor was varied from 12.25 m to 49.0 m. These lengths were chosen to have a ratio for the reactor length to diameter from 3 to 14. By changing the reactor length, the residence time was varied from 16 min to 65 min. Table 1 shows the parameters used for the simulations.

Table 1. Values of the various operating conditions investigated.

Parameter	Value
Reactor diameter, m	3.5
Length, m	12.25, 24.5, 49.0
Temperature, oC	750
Pressure, atm	1
Inlet partial pressure of H ₂	1
Inlet partial pressure of H ₂ O	0
Inlet Partial pressure of N ₂ (inert)	0
Bed void	0.4
Gas flow rate, m ³ /s	31.6
Solid flow rate, Ton/hr (5% Excess)	473.9
Particle diameter, cm	0.50
Particle density, g/cm ³	2.3
Iron loading, Fraction	0.6
Inlet particle conversion	0
Reactor volume, m ³	117.86, 235.72, 471.44
Solid Residence time, min	16.2, 32.4, 64.9

¹ Hydrogen Energy Density = 141.79 MJ/kg (HHV) [Perry's Handbook]

Figure 7 and 8 shows the solid and gas conversions profiles as a function of normalized axial distance for various reactor lengths. In Figure 7 can be seen that above 80% particle conversion can be achieved at the bottom of the reactor ($Z=0$). By increasing the reactor length from 12.25 to 24.5 the solid conversion increased 5%. However, by increasing the reactor length, from 24.5 m to 49.0 m, the solid conversion did not increase significantly. Therefore, according to the simulation, the conversion of the solid at the outlet of the reactor would reach a maximum level when reactor length is beyond a critical value, and this critical length would be the optimized length for the reactor design as it achieves the highest possible conversion under the smallest residence time.

The corresponding hydrogen and water concentration can be seen in Figure 8. As can be seen, the gas conversion go through similar behavior as the solids when increasing the reactor length, where identical outlet/inlet gas concentrations are observed when the reactor length is long enough. After reaching a critical residence time, the increase in reactor length only increases extend the zone in which the reaction rate is low, which can be seen in the middle portion of the reactor. In this zone, the hydrogen concentration is in a near equilibrium with the iron phase present. This pseudo-equilibrium decreases the reaction rate and delay the conversion on the particle. In such zone, the solids and the gas reach a pseudo equilibrium which causes that the overall conversion in the bed to be similar. Hence, the model would help to determine the critical length of the reactor so that an optimized design can be reached.

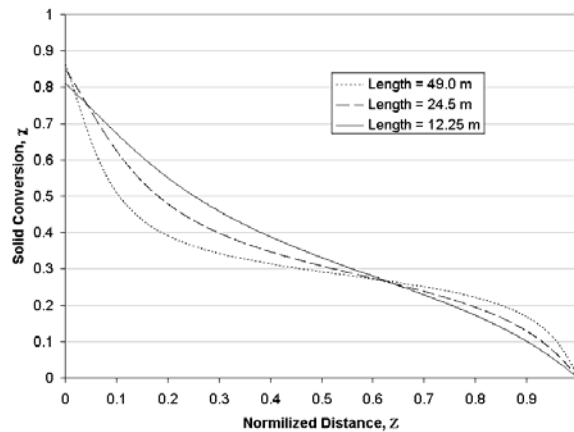


Figure 7. Solid conversion profile for various reactors lengths.

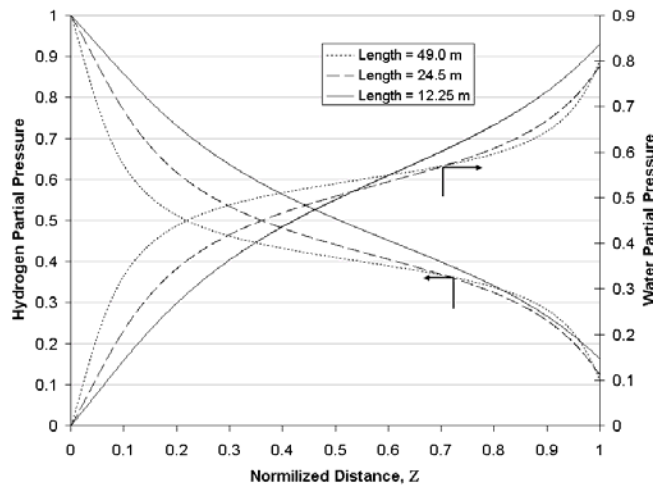


Figure 8. Gas concentration profile for various reactors lengths.

8. Conclusions

The reaction kinetic model was able to predict satisfactory the reduction of iron oxide composite particles, at least for the conditions studied. A moving bed reactor model was constructed, which illustrates the behavior of an industrial scale countercurrent moving bed reactor. It was found that, after a critical reactor length, the conversion did not change significantly. This was due to the particles and the gas reach a condition close to equilibrium in the middle of the reactor creating a near dead zone resulting in similar overall conversions. Hence, the reactor model constructed can be employed in estimating the optimal residence time in the reactor to achieve high conversions with the smallest residence time.

9. Nomenclature

A_c = Reactor cross section

y_{H_2} = Dimensionless hydrogen concentration at the surface of the particle

y_{H_2O} = Dimensionless water concentration at the surface of the particle.

P_{H_2} = Hydrogen partial pressure at the surface of the particle.

$P_{H_2, \text{bulk}}$ = Bulk hydrogen partial pressure

P_{H_2O} = water partial pressure at the surface of the particle.

C_0 = Oxygen concentration.

$C_{0, \text{initial}}$ = Initial Oxygen concentration in the particle.

D = Oxygen diffusion coefficient.

K_e = Equilibrium constant

L = Reactor length

P_t = Total pressure

r = Particle radius.

R = Particle Radii.

S = Dimensionless oxygen concentration.

t = time

Greek Letters

θ = Defined by equation 17.

ϕ = Variation coefficient of diffusion with conversion.

X = Overall particle conversion.

ξ = Dimensionless particle radius.

τ = Dimensionless time.

Z = Dimensionless reactor length

10. Acknowledgments

This work was supported by the Ohio Coal Development Office (OCDO) of the Ohio Air Quality Development Authority (OAQDA).

11. References

Chase, M. W., Jr.; (editor) NIST-JANAF thermochemical *Tables, 4th Ed.*, American Institute of Physics and the American Chemical Society: Woodbury, NY, 1998

Fan, Liang-Shih; Thomas, Theodore J.; Gupta, Puneet; Velazquez-Vargas, Luis Gilberto. Combustion looping using composite oxygen carriers. U.S. Pat. Appl. Publ. 2005175533, 2005

- Fan, L.-S.; Gupta, Puneet; Velazquez-Vargas, Luis G. Methods for making hydrogen from gaseous and solid carbonaceous fuel. U.S. Prov. Pat. Appl. 60/758,507. 2006a.
- Fan, L.-S.; Gupta, Puneet; Velazquez-Vargas, Luis G. Oxygen Carrying Particles for hydrogen via Reduction-Oxidation Reactions and its Synthesis Methods. U.S. Prov. Pat. Appl. 60/758,424. 2006b.
- Fan, L.-S.; Gupta, Puneet; Velazquez-Vargas, Luis G.; Li, F. Syngas chemical Looping Process for Synthesis of Chemicals and Fuels. U.S. Prov. Pat. Appl. 60/808,928. 2006c.
- Fogler H. S. *Elements of chemical reaction engineering*. (1999) Upper Saddle River, N.J. Prentice Hall PTR.
- Herzog Howard. An Introduction to CO₂ Separation and Capture Technologies. 199. http://sequestration.mit.edu/pdf/introduction_to_capture.pdf.
- Lu W.-K., Nabi, G. Reduction kinetics of Hematite to Magnetite in Hydrogen-Water Vapor Mixtures. Transactions of the Metallurgical Society of AIME. 242, 2471-2477, 1968.
- Simbeck, D.; Chang, E. Hydrogen Supply: Cost Estimate for Hydrogen Pathways – Scoping Analysis, USDOE NREL/SR-540-32525, July, 2002
- Stiegel G.J., Ramezan M. Hydrogen from Coal Gasification: An Economical Pathway to a Sustainable Energy Future. International Journal of Coal Geology 2006; 65: 173-190.
- Turkdogan E. T. & Vinters. J. V. Gaseous Reduction of Iron Oxides: Part I. Reduction of hematite in Hydrogen. Metallurgical Transactions. 2, 3175-3188, 1971
- Velazquez-Vargas Luis G., Puneet Gupta, Fanxing Li, L.-S. Fan. Hydrogen Production from Coal derived Syngas Using Novel Metal Oxide Particles. Proceeding, Pittsburgh Coal Conference, 2006.